

7-2012

# Micro-crack ultrasound scattering in anisotropic composite laminates

Ronald A. Roberts

*Iowa State University*, rroberts@iastate.edu

Follow this and additional works at: [http://lib.dr.iastate.edu/cnde\\_conf](http://lib.dr.iastate.edu/cnde_conf)

 Part of the [Materials Science and Engineering Commons](#)

The complete bibliographic information for this item can be found at [http://lib.dr.iastate.edu/cnde\\_conf/7](http://lib.dr.iastate.edu/cnde_conf/7). For information on how to cite this item, please visit <http://lib.dr.iastate.edu/howtocite.html>.

---

This Conference Proceeding is brought to you for free and open access by the Center for Nondestructive Evaluation at Iowa State University Digital Repository. It has been accepted for inclusion in Center for Nondestructive Evaluation Conference Papers, Posters and Presentations by an authorized administrator of Iowa State University Digital Repository. For more information, please contact [digirep@iastate.edu](mailto:digirep@iastate.edu).

---

# Micro-crack ultrasound scattering in anisotropic composite laminates

## **Abstract**

A computational model of ultrasound scattering by micro-cracks in fiber reinforced polymer laminates is presented, foundational to study of micro-crack induced ultrasound attenuation. A model for transmission scattering response is developed using a boundary integral formulation, and associated approximate scattering theories are discussed. Numerical results are presented demonstrating application of the model to laminates containing distributed micro-cracking.

## **Keywords**

QNDE, boundary integral equations, fibre reinforced plastics, laminates, microcracks, ultrasonic absorption, ultrasonic scattering, ultrasonic transmission

## **Disciplines**

Materials Science and Engineering

## **Comments**

Copyright 2013 American Institute of Physics. This article may be downloaded for personal use only. Any other use requires prior permission of the author and the American Institute of Physics.

The following article appeared in *AIP Conference Proceedings* 1511 (2013): 971–978 and may be found at <http://dx.doi.org/10.1063/1.4789149>.

## Micro-crack ultrasound scattering in anisotropic composite laminates

R. A. Roberts

Citation: *AIP Conf. Proc.* **1511**, 971 (2013); doi: 10.1063/1.4789149

View online: <http://dx.doi.org/10.1063/1.4789149>

View Table of Contents: <http://proceedings.aip.org/dbt/dbt.jsp?KEY=APCPCS&Volume=1511&Issue=1>

Published by the [American Institute of Physics](#).

---

### Related Articles

Controllable acoustic media having anisotropic mass density and tunable speed of sound  
*Appl. Phys. Lett.* **101**, 061916 (2012)

Tunable time-reversal cavity for high-pressure ultrasonic pulses generation: A tradeoff between transmission and time compression  
*Appl. Phys. Lett.* **101**, 064104 (2012)

Producing an intense collimated beam of sound via a nonlinear ultrasonic array  
*J. Appl. Phys.* **111**, 124910 (2012)

Formation of collimated sound beams by three-dimensional sonic crystals  
*J. Appl. Phys.* **111**, 104910 (2012)

Contribution of dislocation dipole structures to the acoustic nonlinearity  
*J. Appl. Phys.* **111**, 074906 (2012)

---

### Additional information on AIP Conf. Proc.

Journal Homepage: <http://proceedings.aip.org/>

Journal Information: [http://proceedings.aip.org/about/about\\_the\\_proceedings](http://proceedings.aip.org/about/about_the_proceedings)

Top downloads: [http://proceedings.aip.org/dbt/most\\_downloaded.jsp?KEY=APCPCS](http://proceedings.aip.org/dbt/most_downloaded.jsp?KEY=APCPCS)

Information for Authors: [http://proceedings.aip.org/authors/information\\_for\\_authors](http://proceedings.aip.org/authors/information_for_authors)

### ADVERTISEMENT



AIP Advances

*Submit Now*

Explore AIP's new  
open-access journal

- Article-level metrics now available
- Join the conversation! Rate & comment on articles

# MICRO-CRACK ULTRASOUND SCATTERING IN ANISOTROPIC COMPOSITE LAMINATES

R. A. Roberts  
Center for NDE, Iowa State University, Ames, IA 50014

**ABSTRACT.** A computational model of ultrasound scattering by micro-cracks in fiber reinforced polymer laminates is presented, foundational to study of micro-crack induced ultrasound attenuation. A model for transmission scattering response is developed using a boundary integral formulation, and associated approximate scattering theories are discussed. Numerical results are presented demonstrating application of the model to laminates containing distributed micro-cracking.

**Keywords:** Ultrasonics, Composites, Laminated Structures

**PACS:** 43.35.Yb 43.35.Zc 43.38.Hz

## INTRODUCTION

This paper summarizes model development for quantifying the contribution of elastic wave scattering by matrix micro-cracking to ultrasound attenuation in carbon fiber reinforced polymer (CFRP) composites. Matrix micro-cracking is considered a precursor to a more advanced damage state, hence a means to quantitatively assess levels of micro-cracking would serve early damage detection. Experiments as reported in [1,2] indicate that an increase in ultrasound attenuation accompanies micro-cracking. The present work seeks to determine if the observed attenuation is attributable to linear elastic wave scattering, as opposed to, say, increased non-linear frictional losses. Micro-crack scattering is formulated using boundary integral equation field theory, and solutions are obtained through a combination of numerical and analytical methods. Approximate scattering theories incorporating various levels of multiple scattering are benchmarked against exact problem solutions to establish range of validity. The predictions obtained in this study lend plausibility to the observed increase in ultrasound attenuation being attributable to linear elastic wave scattering.

## MODEL FORMULATION

CFRP laminates of non-woven polymer impregnated fabric are considered in which the reinforcing fiber orientation in successive plies can be uniformly oriented (unidirectional laminate), or vary in a specified ply-to-ply angular pattern (cross-ply laminate). The individual plies are mechanically modeled as homogeneous linearly elastic continua displaying transverse isotropy with symmetry about the reinforcing fiber direction. As such, mechanical properties are specified by mass density  $\rho$  and five independent elastic constants, with stress  $\tau_{ij}$  and displacements  $u_i$  related via the constitutive relation  $\tau_{ij} = c_{ijkl} u_{k,l}$ . Wave motion within the laminate is governed by the elastodynamic field equation, expressed for assumed time harmonic motion with frequency

$\omega$  and applied body forces  $f_i(x)$  as

$$c_{ijkl} u_{k,lj}(x) + \rho\omega^2 u_i(x) = f_i(x) \quad (1)$$

with continuity of displacements and tractions at the ply interfaces imposed as boundary conditions.[3] Laminate matrix micro-cracking introduces the additional boundary condition of zero traction over crack surfaces. Work here reformulates the boundary value problem using elastodynamic reciprocity theory to obtain an equivalent governing boundary integral equation (BIE).[4] Exploiting knowledge of the laminate's response to a singular point body force allows expression of the governing BIE as integrals over the traction free micro-crack surfaces, denoted in total as  $C$ ,

$$\int_C u_i(x) \tau_{ij;k}^G(x|x') n_j(x) dx + \frac{1}{2} u_k(x') = u_k^{inc}(x') \quad , \quad x, x' \in C \quad (2)$$

where  $\tau_{ij;k}^G(x|x')$   $n_j(x)$  is the surface traction in response to a point force  $f_i(x) = \delta_{ik} \delta(x-x')$  acting at position  $x'$  in the  $x_k$  direction within a corresponding crack-free composite laminate (Green state), and  $u_k^{inc}(x')$  is the incident displacement field which would exist in the crack-free laminate. Additional subscripts and argument are included in notating the Green state to identify the location and direction of the applied load. Solutions to eq.(2) are obtained through application of the Boundary Element Method (BEM), which transforms the BIE into a matrix equation by expressing the displacements  $u_i(x)$  as a weighted sum of appropriate basis functions, the solution of which yields the weighting coefficients. The displacement field at position  $x'$  not on a crack surface is expressed in terms of fields on the crack surfaces  $C$  as

$$u_k^{inc}(x') = -\int_C u_i(x) \tau_{ij;k}^G(x|x') n_j(x) dx \quad , \quad x' \notin C \quad (3)$$

The reduction of the boundary value problem to an integral equation defined over the micro-crack surfaces occurs as a consequence of the properties of the Green function, which embodies all propagation behavior of the crack-free laminate. For a laminate of infinite extent with planar ply interfaces, the Green function is formulated using spatial Fourier transformation. Interest in the present work is in the response to a two dimensional point load (a line load if viewed in three dimensions), expressed in Cartesian coordinates as  $f_i(x) = \delta_{ik} \delta(x_1-x_1') \delta(x_2-x_2')$ . As the body force has no  $x_3$  dependence, the resulting fields display no  $x_3$  dependence. Consider first the point load response of an infinite space having the same material properties as the laminate ply hosting the point load, denoted by the superscript "G". Adopting the Cartesian spatial Fourier transform representation for the solution, Fourier integral expressions of the infinite space Green function are obtained

$$\begin{aligned} u_{i;k}^G(x|x') &= \sum_{\alpha} \int \hat{u}_{i;k}^{G\alpha}(k_1|x') \exp(i k_j^{\alpha} x_j) dk_1 \\ \tau_{ij;k}^G(x|x') &= \sum_{\alpha} \int \hat{\tau}_{ij;k}^{G\alpha}(k_1|x') \exp(i k_j^{\alpha} x_j) dk_1 \end{aligned} \quad (4)$$

where  $k_3=0$ , and  $k_2$  is expressed as a function of  $k_1$  through a relation imposed on the wave vector  $k$  by eq.(1). The summation on  $\alpha$  denotes distinct modes of propagation, corresponding to 6 allowable functions  $k_2^{\alpha}(k_1)$ : 3 modes of motion propagating in either  $+x_2$  or  $-x_2$  direction, which along material symmetry axes correspond to longitudinal and two polarizations of shear motion. The integrand of eq.(4) is seen to consist of plane waves multiplied by amplitude coefficients. Procedures in obtaining the expressions of eq.(4) are presented helpful detail in [3]. The response of the laminate structure to the point load is obtained by employing eq.(4) as an incident field on the interfaces bounding the host ply.

It is assumed the laminate consists of  $N$  plies which are sandwiched between two semi-infinite half-spaces of, say, water, air, or transmission wedge material. The system therefore consists of  $N+2$  layers, with  $N+1$  interfaces. Within each ply, fields are expressed as Fourier integrals, as in eq.(4)

$$\begin{aligned} u_i(x) &= \sum_{\alpha} \int \hat{u}_i^{\alpha}(k_1) \exp(i k_j^{\alpha} x_j) dk_1 \\ \tau_{ij}(x) &= \sum_{\alpha} \int \hat{\tau}_{ij}^{\alpha}(k_1) \exp(i k_j^{\alpha} x_j) dk_1 \end{aligned} \quad (5)$$

Within the  $n^{\text{th}}$  ply, the plane wave coefficients in eq.(5) for a given value of  $k_1$  are expressed

$$\begin{aligned} \hat{u}_i^{\alpha n}(k_1) &= a^{\alpha n}(k_1) d_i^{\alpha n}(k_1) \\ \hat{\tau}_{ij}^{\alpha n}(k_1) &= a^{\alpha n}(k_1) t_{ij}^{\alpha n}(k_1) \end{aligned} \quad (6)$$

where  $a^{\alpha n}(k_1)$  is the amplitude of a plane wave with mode type and direction specified by  $\alpha$ ,  $d_i^{\alpha n}(k_1)$  is a unit length displacement vector consistent with the  $\alpha$  wave mode, and  $t_{ij}^{\alpha n}(k_1)$  is the stress field associated with the unit amplitude displacement field of type  $\alpha$ . At each interface, continuity of displacements and tractions requires

$$\begin{aligned} \sum_{\alpha} a^{\alpha n}(k_1) d_i^{\alpha n}(k_1) &= \sum_{\alpha} a^{\alpha n+1}(k_1) d_i^{\alpha n+1}(k_1) \\ \sum_{\alpha} a^{\alpha n}(k_1) t_{i2}^{\alpha n}(k_1) &= \sum_{\alpha} a^{\alpha n+1}(k_1) t_{i2}^{\alpha n+1}(k_1) \end{aligned} \quad (7)$$

where  $i=1,2,3$ , and  $n=0, \dots, N$ . Plies  $n=0$  and  $n=N+1$  correspond to the surrounding semi-infinite half-spaces. A determined system of equations for field amplitude coefficients  $a^{\alpha n}(k)$  is obtained by imposing that fields in the surrounding half spaces propagate away from the laminate.

The response of the laminate to the point load acting in the  $m^{\text{th}}$  ply is obtained by employing eq.(4) as an incident field on the interfaces bounding the  $m^{\text{th}}$  ply in eq.(7)

$$\begin{aligned} \sum_{\alpha} a^{\alpha n} d_i^{\alpha n} + \delta_{nm} \sum_{\alpha+} \hat{u}_{i:k}^{G\alpha}(x') &= \sum_{\alpha} a^{\alpha n+1} d_i^{\alpha n+1} + \delta_{n+1m} \sum_{\alpha-} \hat{u}_{i:k}^{G\alpha}(x') \\ \sum_{\alpha} a^{\alpha n} t_{i2}^{\alpha n} + \delta_{nm} \sum_{\alpha+} \hat{\tau}_{i2:k}^{G\alpha}(x') &= \sum_{\alpha} a^{\alpha n+1} t_{i2}^{\alpha n+1} + \delta_{n+1m} \sum_{\alpha-} \hat{\tau}_{i2:k}^{G\alpha}(x') \end{aligned} \quad (8)$$

where the summation over  $\alpha+$  or  $\alpha-$  denotes inclusion of wave modes propagating in the  $+x_2$  or  $-x_2$  directions, respectively, and  $k_1$  dependence is implied. The Green function response is evaluated by performing a numerical integration of eq.(5), for which the integrand at each value of  $k_1$  is obtained as the solution to eq.(8). The numerical integration employs complex  $k_1$  contour deformation to accelerate numerical convergence.

A special case is the unidirectionally reinforced composite, for which material elastic properties are uniformly orientated in all plies. In this case, there are effectively no ply boundaries. Furthermore, imposition of planar perpendicular longitudinal incidence results in the restriction of displacements to two dimensions, in which case the problem cannot be distinguished from a corresponding two-dimensional scattering problem in a fully isotropic infinite space. A substantial simplification in problem formulation and subsequent computation arises as a consequence.

Ultrasonic attenuation is perceived as a reduction in transducer output voltage upon reception of a transmitted pulse. Model predictions of receiver output voltage are obtained through application of Auld's reciprocity relation, which relates generated and received wave fields to input and output transducer voltages.[5] Specifically, Auld's relation

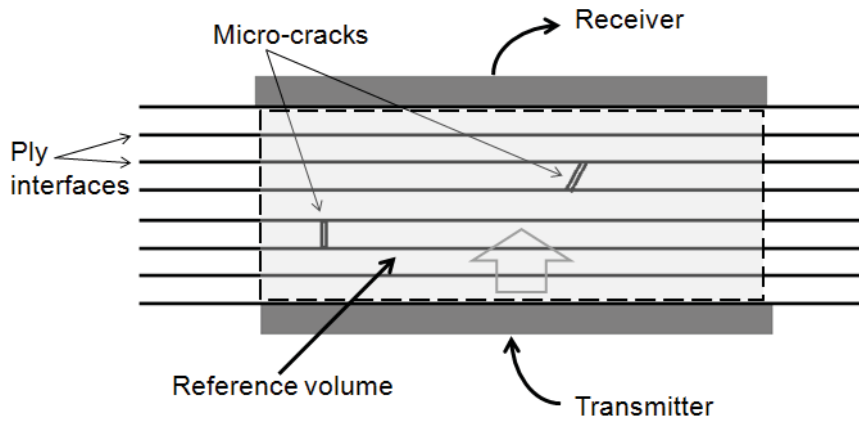


**FIGURE 1.** Configuration of computational model.

expresses the change in receiver output voltage  $\delta v$  due to introduction of a wave field on a specified surface arising from a transmitting transducer. For the micro-crack problem this relation is expressed

$$\delta v = \Gamma \int_C u_i(x) \tau_{ij}^{\text{rec}}(x) n_j(x) dx \quad (9)$$

where  $u_i(x)$  is the displacement field on the crack surfaces  $C$  resulting from interaction with a field generated by a transmitting transducer, and  $\tau_{ij}^{\text{rec}}(x)$  is the stress which would exist at the crack locations in the absence of the cracks were the receiver is used reciprocally as a transmitter. The factor  $\Gamma$  represents among, other things, the electro-mechanical conversion efficiency of the transducers.

The experimental configuration considered is depicted in fig.(1). A transmitter and receiver are positioned on opposing sides of a composite laminate, containing some number of micro-cracks. Longitudinal motion transducers are assumed, i.e., were the transducers infinite in extent, they would generate a longitudinal plane wave emerging perpendicular to the transducer face. When considering finite dimensions, the transducers additionally generate and receive edge diffracted signals. The dimension of the receiving transducer is prescribed to cover a reference volume of composite material into which micro-cracks are distributed. The transmitter is assumed to be as large as (or larger than) the receiver. Simplifying assumptions are made in applying the BIE/BEM analysis to the configuration of fig.(1). First, to eliminate reverberation between outer laminate surfaces, it is assumed that the composite laminate is infinite in extent, and is sandwiched between two half-spaces of unidirectional composite, where the material orientation of the neighboring half-spaces matches that of the adjacent laminate surface plies. Second, the incident field generated by the transmitter is assumed to be an ideal plane wave of longitudinal motion propagating perpendicular to the ply interfaces. Lastly, when evaluating the output voltage contribution generated by motion of the crack faces, eq.(9), the reciprocally generated receiver field is likewise assumed to be an ideal longitudinal plane wave, propagating opposite the incident field. Broadband temporal responses are of experimental interest, therefore computed time harmonic responses are Fourier transformed assuming an experimentally relevant transducer frequency response.

Micro-cracks are observed to occur in the matrix between reinforcing fibers, thereby running parallel to the fibers, and extend between neighboring ply interfaces. A micrograph showing matrix micro-cracking can be seen in [2]. To keep the scope of the computation supportable by a laptop PC, the BIE analysis is limited to a 2D field dependency. To this end, the micro-cracks are assumed infinite in length, and all aligned in the same direction. Consequently, the formulation is applicable to uni-directionally

reinforced laminates, and cross-ply laminates for which micro-cracks are only located in plies of a particular orientation. Under this restriction, it is seen that, although motions can be three dimensional, the spatial dependency of the motion will display no dependency on the crack length direction.

The application of BEM analysis to eq.(2) is now discussed in more detail. A volume of composite laminate is assumed to contain a number of micro-cracks, and all cracks are aligned with the  $x_3$  coordinate axis. Fields therefore depend only on  $x_1, x_2$  coordinates, where the  $x_2$  coordinate is perpendicular to the ply interfaces. The  $x_1$ - $x_2$  cross-section of each crack surface is divided into adjacent intervals, and displacements  $u_i(x)$  are approximated by to-be-determined constant values over each interval. Employing this prescribed form for the displacement field into eq.(2), and evaluating eq.(2) at positions  $x'$  located at the center of each interval leads to a matrix equation for the sought piece-wise constant values of  $u_i(x)$ . Inversion of the matrix equation yields the exact determination (in the numerically convergent sense) of the crack surface displacements, fully accounting for all multiple crack scattering interactions. The BEM matrix to be inverted following such a procedure can become quite large when there are many (e.g. hundreds) of cracks contained in the reference volume.

Approximate multiple scattering theory considers scattering interactions between cracks as sequential events. Considering cracks individually, eq.(2) can be rewritten

$$\int_{C_m} u_i(x) \tau_{ij;k}^G(x|x') n_j^m(x) dx + \frac{1}{2} u_k(x') = u_k^{inc}(x') - \sum_{n \neq m} \int_{C_n} u_i(x) \tau_{ij;k}^G(x|x') n_j^n(x) dx \quad (10)$$

where the subscript on C identifies a particular crack. Restricting  $x'$  to crack surface  $C_m$ , eq.(10) can be viewed as an integral equation for determining the displacement on crack  $C_m$ , provided the displacements are known on all other cracks. The integrals on the right hand side thereby become an addition to the incident field seen by crack  $C_m$ . Approximate scattering theory proceeds in an iterative process, expressed

$$\int_{C_m} u_i^{p+1}(x) \tau_{ij;k}^G(x|x') n_j^m(x) dx + \frac{1}{2} u_k(x') = u_k^{inc}(x') - \sum_{n \neq m} \int_{C_n} u_i^p(x) \tau_{ij;k}^G(x|x') n_j^n(x) dx \quad (11)$$

where displacements  $u_i^p(x)$  represent different levels of scattering interaction. The 0<sup>th</sup> level field is prescribed as the incident field, for which case  $u_i^0(x)=0$ . The 1<sup>st</sup> level field  $u_i^1(x)$  is obtained by solving eq.(11) for all  $C_m$  with  $p=0$ . The 1<sup>st</sup> level field accounts for the scattering of the incident field, as if neighboring cracks were not present, commonly referred to as the independent scattering approximation. Solving eq.(11) for all  $C_m$  with  $p=1$ , and using the 1<sup>st</sup> level fields in the right hand side yields the 2<sup>nd</sup> level field, which accounts for the scattering of the initial scattering from neighbors. Higher level fields are sequentially obtained for  $p=2, 3$ , and so on.

The general case of micro-crack scattering in cross-ply composites in which cracks are contained in non-aligned plies cannot be solved as a 2D scattering problem, due to a full 3D spatial dependence of the resulting scattered wave fields. However, the 2D analysis described above can be utilized to obtain 1<sup>st</sup> and 2<sup>nd</sup> level approximate multiple scattering predictions in the general cross-ply case. The 1<sup>st</sup> level scattering contribution is readily obtained in the general cross-ply configuration for which scattering is individually considered for each crack. 2<sup>nd</sup> level and higher contributions are also readily obtained for interactions between similarly oriented cracks. For cracks in neighboring plies oriented at non-zero angle, an approximation for 2<sup>nd</sup> level interaction is derived by taking the receiver field in eq.(9) to be the 1<sup>st</sup> level scattered field resulting from reciprocal use of the receiver

as a transmitter. The 1<sup>st</sup> level scattered field generated by a crack  $C_m$  is evaluated at points  $x'$  within the laminate using eq.(4), where the displacement  $u_i(x)$  on  $C_m$  results from scattering of the receiver field. Employing eq.(9) in eq.(3) yields as the contribution of the scattering of the incident field by crack  $C_n$  in turn scattering from crack  $C_m$

$$\delta v = -\Gamma \int_{C_n} u_i^n(x') c_{ijkl} \int_{C_m} u_p^m(x) \tau_{pq;kl}^G(x|x') n_q^m(x) dx n_j^n(x') dx' \quad (12)$$

where  $u_i^n(x)$  is the displacement resulting from scattering of the transmitter field, and  $u_i^m(x)$  is the displacement resulting from scattering of the receiver field. It is noted that both the displacements and the Green function in eq.(12) display 2D spatial dependence, but since the cracks are not aligned, the argument of the Green function varies with distance along crack length. Importantly, all quantities in eq.(12) are readily evaluated. Rather than performing a surface integration (a 2D surface in 3 dimensions) over both cracks, it is noted that the phase dependence of the Green function displays stationary behavior at the shortest distance between the crossing cracks. The integrations along the length of the crack are therefore evaluated using a stationary phase asymptotic analysis. The remaining integrals thereby require a line integration around the crack  $C_m$  cross-section at the stationary point (the crack crossing point viewed from the  $x_2$  direction), and a corresponding line integration around the crack  $C_n$  cross-section at the stationary point.

Attenuation is observed experimentally as a reduction in through-transmitted pulse amplitude. The receiving transducer signal contribution provided by eq.(9) provides the signal arising from forward scattering by the cracks which subtracts from the crack-free transmitted signal through phase cancelation. The signal received in the absence of micro-cracking is evaluated by applying Auld's reciprocity relation over the surface  $R$  of the receiving transducer, expressed

$$\delta v = \Gamma \int_R (u_i^{tr}(x) \tau_{ij}^{re}(x) - u_i^{re}(x) \tau_{ij}^{tr}(x)) n_j(x) dx \quad (13)$$

where the superscripts "tr" and "re" denote fields associated with the transmitter and receiver. Evaluating eq.(13) assuming transmitter and receiver fields are both ideal plane waves results in an infinite output voltage, due to the infinite extent of the receiver. A meaningful result is obtained by restricting the receiver area  $R$  to the size of the reference volume in fig.(1) into which the micro-cracks are introduced. It is noted that using the same finite-sized receiver in the evaluation of eq.(9) results in the introduction of edge diffracted signals in the receiver output. Upon examining broad-band signal transmission, it is observed that these edge diffracted signals by-and-large arrive after the initial forward scattered signal, and therefore do not come into play in determining the amplitude of the total through transmitted pulse, obtained as the sum of eqs.(9 and 13).

## NUMERICAL RESULTS

The formulation described above is applied to predict the through-transmission scattering response to micro-cracks contained in CFRP composite laminates. Elastic constants of the transversely isotropic plies are prescribed, using Voigt notation, as  $C_{11}=12.3$ ,  $C_{12}=6.25$ ,  $C_{13}=5.94$ ,  $C_{33}=175.0$ ,  $C_{44}=5.29$ , in GPa units, where a local ply coordinate system is assumed to have  $x_3$  as the material symmetry axis, and density is assigned  $\rho=1.57E3$  kg/m<sup>3</sup>. A ply thickness of 0.16mm is prescribed.

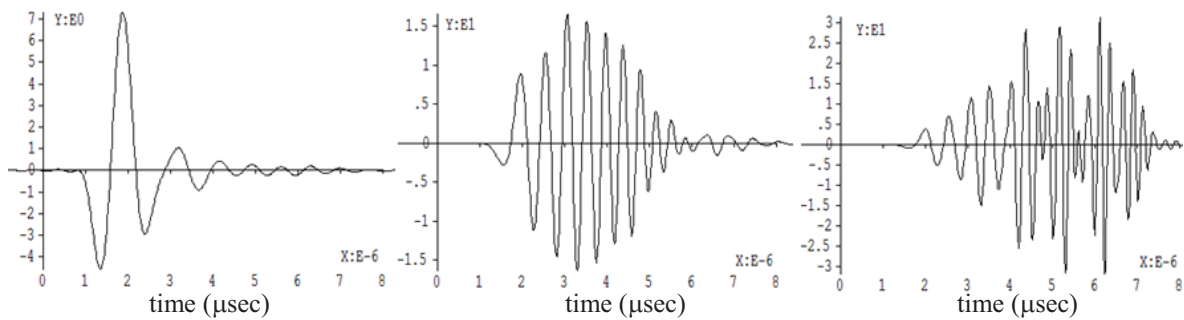


**FIGURE 2.** Temporal Green function response at 3.2 mm: a) 0.875 MHz, b) 1.75 MHz, c) 3.5 MHz.

Results are first shown demonstrating the evaluation of the Green state for a point load applied in a host ply. A 15 ply laminate is considered in a 0,45,90,-45 degree layup, sandwiched by half-spaces of unidirectional composite with orientation matching the outer laminate layers, so as to eliminate reflection from the outer laminate surfaces. A line load is applied in the center of the center layer, which has its fiber orientation in the  $x_3$  direction. A broad-band temporal response is assumed, have a 100% bandwidth Hanning window frequency spectrum. Expressions for Green state displacement  $u_{i;k}^G(x|x')$  given by eqs.(4-8) are evaluated using a numerical  $k_1$  contour integration which optimally exploits the source-to-observation distance to accelerate numerical convergence. Time harmonic motions are then multiplied by the specified frequency spectrum and Fourier transformed to yield temporal responses as plotted in fig.(2). The  $u_{1;1}$  response observed at a distance of 20 ply thicknesses in the  $x_1$  direction is plotted in fig.(2) for center frequencies of 0.875 MHz, 1.75 MHz, and 3.5 MHz. It is seen that these frequencies cover the range over which the response transitions from that of a homogeneous medium to that of a layered structure. As experiments are modeled at 3.5 MHz, the response observed in fig.(2) indicates the need to treat the laminate as a layered structure, rather than approximating its elastic properties by an effective homogeneous medium.

An example of application to scattering by a distribution of micro-cracks in a 16 ply unidirectional laminate is presented, where 112 cracks are randomly distributed in a 4.85 mm wide volume (320 cracks/cm) using an algorithm described in [2]. The micro-cracks are assumed perpendicular to and extend between neighboring ply interfaces. A 3.5 MHz center frequency pulse is transmitted through the volume, and the receiver output is evaluated. The signal output in the absence of cracks is scale to unity. Level 1 (independent scattering) and level 2 scattering predictions are compared to the exact fully-interacting scattering prediction in fig.(3). The level 1 scattering prediction is seen to significantly under-predict the scattering induced attenuation at this crack density, whereas the level 2 prediction is in substantially better agreement with the exact value. A feature which is noticeably absent in the level 1 prediction is the noise tail arising from multiple crack scattering interactions. The level 2 result displays a multiple scattering noise tail, but is seen to over-predict its amplitude at later times. Calculations as demonstrated in fig.(3) were performed over a range of crack densities, and predicted output signals were used to estimate scattering induced attenuation as a function of crack density. Results of this numerical study are presented in [2]. In that study, the limits of validity of the various approximate multiple scattering theories are examined, in both unidirectionally reinforced and cross-ply composites. That study also compares numerical predictions obtained using the modeling approach presented here to predictions obtained by an alternative finite difference based computation, in which agreement was confirmed.

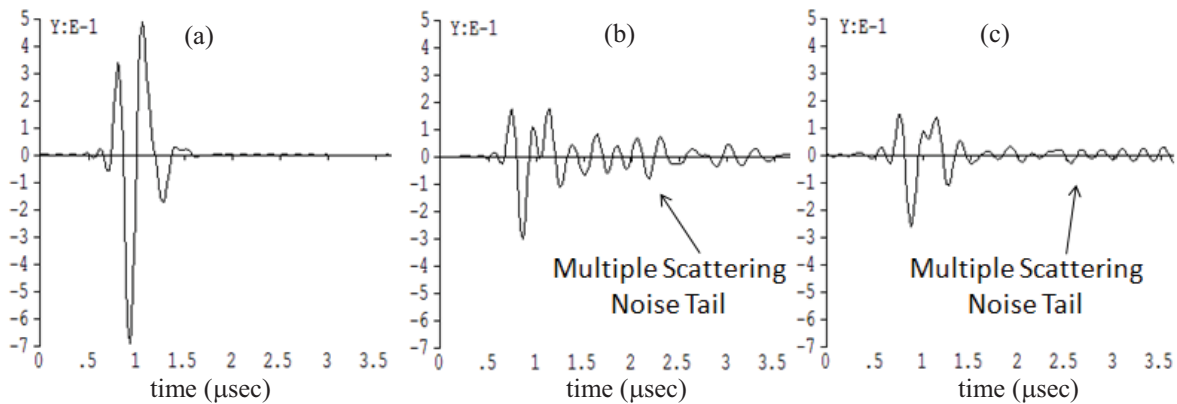


**FIGURE 3.** Transmitted signals for crack density of 320 micro-cracks/cm: a) level 1 approximation (independent scattering), b) level 2 scattering (single neighbor interaction), c) fully interacting exact BEM inversion.

## SUMMARY

A model formulation is presented for predicting received ultrasound signals upon transmission through CFRP composite laminates containing distributed micro-cracking. Using elastodynamic reciprocity theory, a boundary integral equation (BIE) representation of crack surface motion induced by pulse transmission is obtained, which is solved in either exact or approximate fashion using boundary element method (BEM) analysis. The BIE formulation exploits the Green state response of the corresponding crack-free laminate. The analysis and numerical procedures used to evaluate the Green state response for a general cross-ply CRFP laminate are summarized and demonstrated. The derivation is summarized of approximate multiple scattering methods which obtain crack surface motions as a sequence of crack interactions, with successive levels of interaction producing corresponding approximate theories, the first level being the independent scattering approximation. Numerical results are presented comparing first and second level scattering theories to exact prediction for a selected case of distributed micro-cracking in a composite laminate. The model formulation and numerical procedures summarized here are employed in a companion paper to study the prediction of ultrasound attenuation as a function of micro-crack density.[2]

## ACKNOWLEDGEMENT

This work is supported by NASA under award NAG-1-029098.

## REFERENCES

1. C.A.C. Leckey, M.D. Rogge and F.R. Parker, "Micro-Cracking In Composite Laminates: Simulation Of Crack-Induced Ultrasound Attenuation," *these proceedings*.
2. R. Roberts and C.A.C. Leckey, "Computational Modeling Of Micro-Crack Induced Attenuation In CFRP Composites", *these proceedings*.
3. J. Achenbach, *Wave Propagation in Elastic Solids*, Elsevier, 1982.
4. J. Achenbach, *Reciprocity In Elastodynamics*, Cambridge, UK, 2003.
5. B. Auld, "General Electromechanical Reciprocity Relations Applied to the Calculation of Elastic Wave Scattering Coefficients," *Wave Motion* Vol. 1, 1979.